In Vitro Antifungal, Anticancer Activities and POM Analyses of a Novel Bioactive Schiff Base 4-{[(*E*)-furan-2-ylmethylidene]amino}p-henol: Synthesis, Characterization and Crystal Structure

[1]Said Tighadouni, [1]Smaail Radi, [2]Muhammad Sirajuddin*, [3]Mehmet Akkurt, [4]Namık Özdemir
[5]Matloob Ahmad, [6]Yahia N. Mabkhot and [7]Taibi Ben Hadda**
[1]*LCAE, Département de Chimie, Faculté des Sciences, Université Mohammed Premier, Oujda 60000, Morocco.*
[2]*Department of Chemistry, University of Science & Technology, Bannu Pakistan.*
[3]*Department of Physics, Faculty of Sciences, Erciyes University, 38039 Kayseri, Turkey.*
[4]*Department of Physics, Faculty of Arts and Sciences, Ondokuz Mayıs University, 55139 Samsun, Turkey.*
[6]*Department of Chemistry, College of Science, King Saud University, P. O. Box 2455, Riyadh-11451, Saudi Arabia.*
[7]*Laboratoire de Chimie des Matériaux, Faculté des Sciences, Université Mohammed Premier, Oujda 60000, Morocco.*
m.siraj09@yahoo.com , taibi.ben.hadda@gmail.com

(Received on 12th June 2015, accepted in revised form 7th October 2015)

Abstract: The title compound (**1**), $C_{11}H_9NO_2$, was synthesized and characterized by FT-IR, ^1H NMR, ^{13}C NMR spectroscopy, mass spectrometry and single crystal analysis. It was crystallized in a monoclinic system with a space group $P2_1/n$. The dihedral angle between the planes of furan and benzene ring is 21.24 (11)°. The torsion angle of bridge –C—C—N—C–is -177.81(15)°. The crystal structue is stabilized by intermolecular hydrogen bonds between O—H...N and C—H...O forming a three dimensional network. The synthesized compound was screened for the *in vitro* antifungal against the *Fusarium oxysporum f.sp albedinis FAO* fungal strains and showed good activity. It was also tested for the anticancer activities against breast (MDA-MB231) and colorectal (LOVO) cancer cell lines and exhibited IC_{50} values of 6.9 µg/mL and 14.6 µg/mL, respectively. POM calculations of molecular properties of **1** are in good agreement with the mode of antifungal action of the compound bearing ($X^{\delta-}$---$Y^{\delta-}$) pharmacophore site. Also it shows a drug score of 43% which is an important parameter for the compound possessing the drug character.

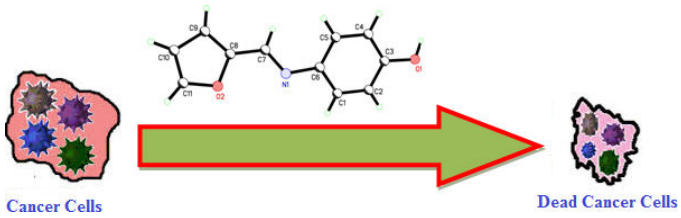

Keywords: NMR; Crystal Structure; Antifungal activity; Anticancer activity; POM analysis.

Introduction

Schiff bases represent one of the most widely used classes of organic compounds, not only as synthetic intermediates but also in coordination chemistry. Schiff bases derived from an amino and carbonyl compound are an important class of ligands that coordinate to metal ions *via* imine (azomethine) nitrogen and have been studied extensively. In Schiff base derivatives, the C=N linkage is vital for biological activity. Schiff bases derived from sulfane thiadizole and salicylaldehyde or thiophene-2-aldehydes and their complexes show toxicities against insects. α-Aminoacid acts as intermediate in synthesis of photostable pyrthriod insecticides [1]. Schiff bases are an important class of compounds both in medicinal and pharmaceutical fields [2, 3] and have also been found to exhibit a broad range of biological activities including antifungal, antibacterial, antimalarial, antiproliferative, antiinflammatory, antiviral, and antipyretic properties [4, 5]. Especially, hydroxyl-substituent Schiff bases, because the attachment of hydroxyl groups on the aromatic ring makes the compound a free-radical scavenger, hydroxyl-substituent Schiff bases may be antioxidants to scavenge free radicals, and potential drugs to treat diseases related to free-radical damage [6].

*To whom all correspondence should be addressed.

Keeping in mind the bioactivity of Schiff bases, a novel Schiff base bearing furan and thiophen rings has been synthesized and evaluated for the *in vitro* antifungal activity against *Fusarium oxysporum f.sp albedinis FAO* fungal strains and the anticancer activity toward breast (MDA-MB231) and colorectal (LoVo) human cell lines cancers.

Experimental

Materials and Measurements

All solvents and chemicals obtained from usual commercial sources, were of analytical grade and used without further purification. FT-IR spectrum was performed on a FT-IR Paragon 500 Perkin-Elmer et FT-IR System 2000 Perkin-Elmer, IUT de Blois-Université François Rabelais (France). The ^{1}H NMR spectra were obtained with a Bruker AC 300 spectrometer. The Molecular weights were determined on a JEOL JMS DX-300 Mass Spectrometer. The X-ray diffraction data was performed on a STOE IPDS 2 diffractomer employing graphite-monochromated Mo-Kα radiation generated from a fine-focus sealed tube (λ = 0.71073 Å) at room temperature. Data collection strategy was evaluated by using the X-AREA software [7] in the ω scan mode. The data was corrected by absorption effects with X-RED32 [8] using the integration technique. The structure was solved by direct methods using SHELXS-97 [9] and refined by least-squares methods on F^2 using SHELXL-97 [9]. All non-hydrogen atoms were refined with anisotropic parameters. H atoms were positioned geometrically and were refined using a riding model with $U_{iso}(H) = 1.5U_{eq}(O)$ for hydroxyl group and $U_{iso}(H) = 1.2U_{eq}(C)$ for the other. Molecular drawings were performed using PLATON [10]. Geometric calculations were performed with PLATON [10].

Synthesis of (E)-4-(furan-2-ylmethyleneamino)phenol (**1**)

A solution of furan-2-carbaldehyde (2 g, 20.3 mmol) was dissolved in dried diethyl ether (15 mL) and was added to a solution of 4-aminophenol (2.3 g, 20.3 mmol) which was already dissolved in dried diethyl ether (90 mL). The mixture was stirred at room temperature for 8 days using a few drops of acetic acid as catalyst. The formed product was filtrated and washed with dried ether. The final purification was performed by re-crystallization from hot methanol [11]. The chemical reaction is shown in Scheme 1.

Pink powder. Yield 63.15% (2.4 g, 12.82 mmol). M.p. 197-199 °C. R_f = 0.5 (silica, CH_2Cl_2/ MeOH, 9/1). IR: ν(CH=N, imine) = 1630 cm^{-1}; ν (OH) = 3250 cm^{-1}; ν(N-$H_{stretching}$) = 3470 cm^{-1}; ν(N-$H_{bending}$) = 1437 cm^{-1}; ν(C-N) = 1290 cm^{-1}: ^{1}H NMR (300 MHz, DMSO) δ ppm: 7.86 (d, 1H, H1, $^3J[^1H$-$^1H]$ = 1.5 Hz); 6.65 (t, 1H, H2, $^3J[^1H$-$^1H]$ = 3.6 Hz); 7.03 (d, 1H, H3, $^3J[^1H$-$^1H]$ = 3.6 Hz); 8.39 (s, 1H, H5); 7.15 (d, 2H, C7,C7', $^3J[^1H$-$^1H]$ = 3.9 Hz); 6.77 (d, 2H, C8,C8', $^3J[^1H$-$^1H]$ = 6.9 Hz); 9.52 (s, 1H, OH). ^{13}C NMR (75 MHz, DMSO) δ ppm: 146.2 (C1); 112.8 (C2); 116.2 (C3); 152.8 (C4); 145.6 (C5); 142.8 (C6); 122.9 (C7, C7'); 115.9 (C8, C8'); 156.8 (C9). m/z (M^+): 188.21.

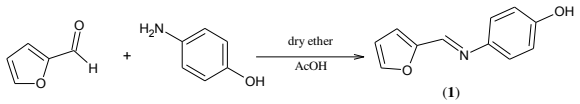

(**1**)

Scheme-1: Synthesis of (*E*)-4-(furan-2-ylmethyleneamino) phenol (**1**)

Antifungal Activity Assay

The *in vitro* antibacterial and antifungal activity were tested by the agar diffusion technique (ADT) [12]. ADT has been investigated using susceptibility test of NCCLS (National Committee for Clinical Laboratory Standards) recommended by the WHO and the French standard NF - U - 47-107 AFNOR 2004. The agar media were inoculated with test organisms and a solution of the tested compound in DMSO/EtOH (50/50) was added to different concentration in the culture media. The growth was followed by a count of bacteria and yeast colonies and measurement of mycelium diameter. The inhibition percentage of a molecule is equal to the ratio of the colonies number or the mycelium diameter of the culture in the presence of a dose of the tested compound over the colonies number or the mycelium diameter of the reference culture multiplied by 100. The minimum inhibition concentration (MIC) is the least dose of the compound which caused inhibition of the micro organism growth.

Calculation the concentration IC_{50} was done using the same bacterial inocula mentioned above with decreasing concentration of the tested products. D_o was measured of each culture at 625 nm.

$$\% \text{ Inhibition} = \frac{D_{o-D_x}}{D_o} \times 100 \qquad \text{(Eq.1)}$$

D_o = Diameter of the mycelial growth of the culture witness
D_x = Diameter of the mycelial growth in the presence of the product to be tested

Anticancer Activity Assay

The synthesized compound was evaluated for anticancer activity against breast (MDA-MB231) and colorectal (LoVo) human cancer cell lines using MTT protocol [13]. MTT tests were performed in order to rapidly, i.e., within 3 days, measure the effect of compounds on the overall cell growth. The test measures the number of metabolically active living cells that are able to transform the yellow product 3-(4,5-dimethylthiazol-2-yl)-2,5-diphenyl tetrazolium bromide (herein referred as MTT) into the blue product formazan dye by mitochondrial reduction. The amount of formazan measured by a spectrophotometer (Plate Reader Victor X4 Microplate reader (Perkin Elmer), is directly proportional to the number of living cells. To perform the assay, cells were allowed to grow in 96-well microplates with a flat bottom following addition of an amount of 100 µL of cell suspension per well with 4,500 cells/well. Cell lines were seeded in Glutamax-containing RPMI supplemented with 10% Fetal Bovine Serum (PAA) and 1% penicillin + streptomycin mix (Invitrogen). The detailed experimental procedure was as following: after a 24 h period of incubation at 37°C, the culture medium was replaced by 100 µL of fresh medium in which the tested compound was previously dissolved at the following concentrations: 1×10^{-8}, 5×10^{-8}, 1×10^{-7}, 5×10^{-7}, 1×10^{-6}, 5×10^{-6}, 1×10^{-5}, 5×10^{-5} and 1×10^{-4} g/mL. Each experiment was performed in sestuplicates. Cells were then incubated at 37°C in a Binder incubator under 5% CO_2-containing humidified atmosphere.

After 72 h of incubation, with or without the compound to be tested, the medium was replaced by 100 µL of HBSS (without phenol red) containing MTT at a concentration of 1 mg/mL. The micro-wells were subsequently incubated for 3 h at 37°C and centrifuged at 1300 rpm during 10 min. Medium was removed and formazan crystals formed were dissolved in 100 µL DMSO. The micro-wells were shaken for 5 min and read on a spectrophotometer at wavelengths of 570 nm (maximal formazan absorbance) [11, 14].

For each experimental condition, the mean optical density was calculated to determine the percentage of living cells in comparison to the control.

Petra/ Osiris/Molinspiration (POM) analyses

Petra/Osiris/Molinspiration analysis (POM) is one of the well known approaches that has been used regularly to produce the two dimensional models to identify and ndicate the type of pharmacophore site that affects biological activity with a change in the chemical substitution. The advantages of POM are the ability to predict the biological activities of the molecules and to represent the relationships between steric/electrostatic property as well as biological activity in the form of pharmacophore site, which gives key features on not only the ligand-receptor interaction, but also on the topology of the receptor [15].

Results and Discussion

FT-IR

In the FT-IR spectrum of compound **1,** a sharp band observed at 3250 $cm^{-1}$was assigned to free O–H. A strong band attributable to C=N was observed at 1630 cm^{-1}. The stretching vibration of medium intensity for N-H band occured at 3470 cm^{-1} while a weak intensity peak for bending vibration of N-H was observed at 1430 cm^{-1}. A peak of medium intensity assigned to the stretching vibration of N-C band occured at 1290 cm^{-1} [16-18]. The detail of IR result was given in experimental section.

NMR

The NMR spectrum of compound **1** was recorded in d^6-DMSO. The ^{1}H NMR spectrum was shown in Fig. 1. The chemical shifts of the different types of protons and carbons are given in experimental part. The formation of compound **1** was supported by the appearance of a sharp singlet corresponding to the iminie proton (-N=CH-) at 8.39 ppm. The hydroxyl proton in compound **1**showed a broad singlet at 9.52 ppm [16-18].

In the ^{13}C NMR spectrum of compound **1,** the peak at 152.8 ppm belongs to the imine carbon (C=N) [16-18]. The remaining peaks are described in the same positions as calculated by incremental methods. The ^{13}C NMR spectrum is shown in Fig. 2.

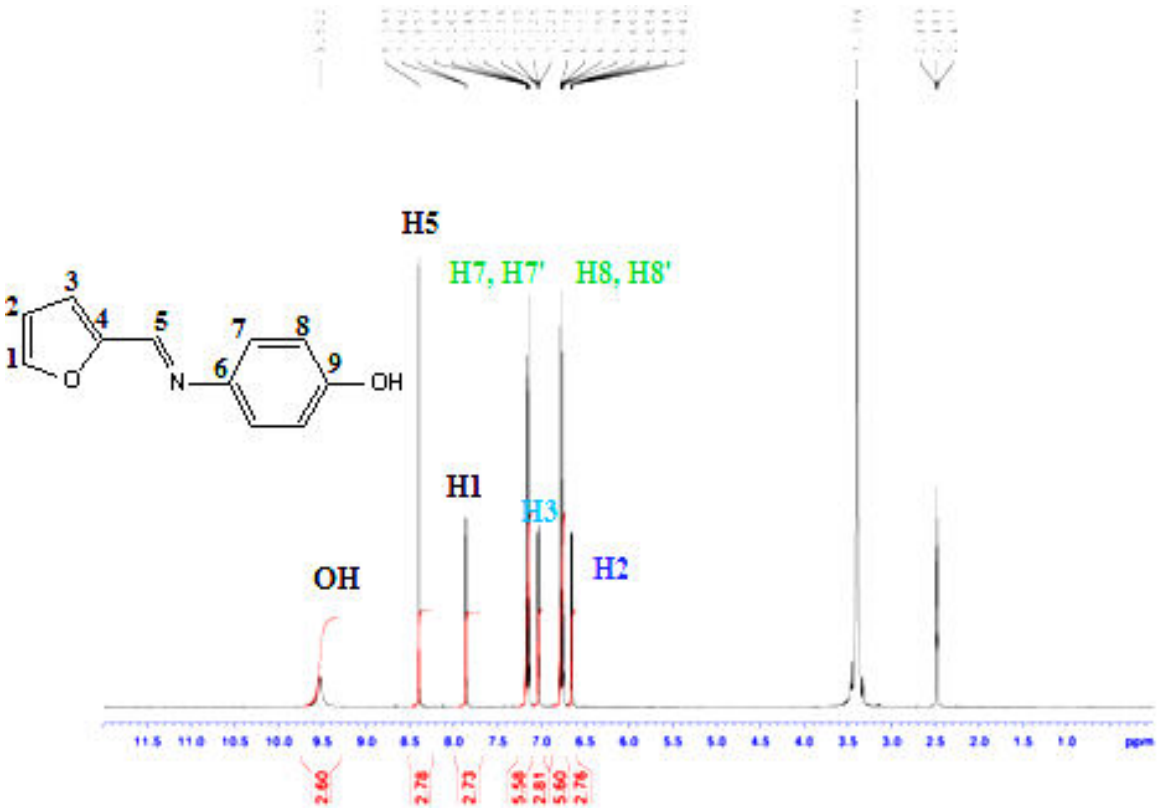

Fig. 1: ^{1}H NMR spectrum of compound **1.**

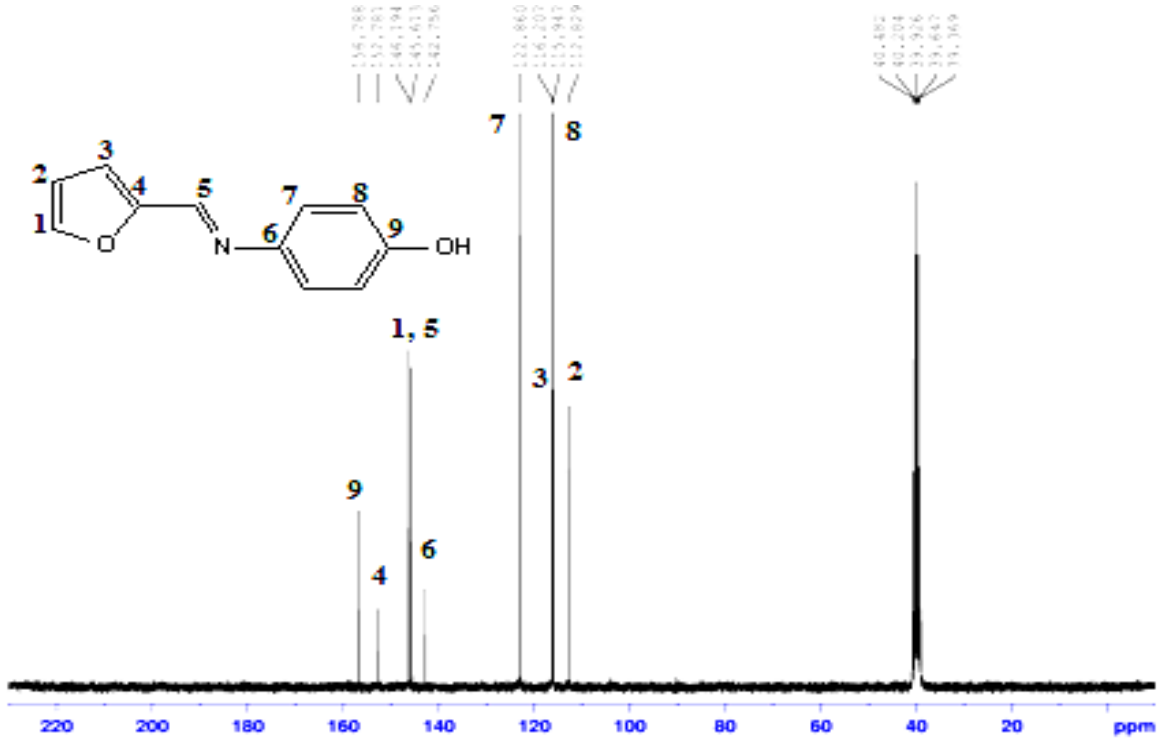

Fig. 2: ^{13}C NMR spectrum of compound **1.**

Mass Spectrometry

The MS spectrum of the synthesized comppound **1** was shown in Fig. 3. The compound showed a molecular ion peak (parent peak) of maximum intensity with m/z = 188.21. This might be due the isotopic nitrogen (^{15}N). M+1 peak was also observed with intensity of 15.

X-ray Structure Determination of **(1)**

Table-1: Crystal and experimental data of **1.**

Chemical formula	**$C_{11}H_9NO_2$**
M_r	**187.19**
Crystal system, space group	**Monoclinic, $P2_1/n$**
Temperature (K)	**296**
a, b, c (Å)	**6.2602 (5), 13.2494 (9), 11.3050 (9)**
α, β, γ (°)	**90.000, 93.167 (6), 90.000**
V (Å^3)	**936.25 (12)**
Z	**4**
F(000)	**392**
D_x (mg m^{-3})	**1.328**
Radiation type	**Mo Kα**
No. of reflections for cell measurement	**8664**
2θ range (°) for cell measurement	**1.8–28.0**
μ (mm^{-1})	**0.09**
Crystal shape	**Prism**
Colour	**Pale yellow**
Crystal size (mm)	**0.51 × 0.47 × 0.40**
Absorption correction	**Integration**
T_{min}, T_{max}	**0.961, 0.975**
No. of measured, independent and observed [I > 2σ((I)] reflections	**7499, 2148, 1450**
R_{int}	**0.099**
θ values (°)	**θ_{max} = 27.6, θ_{min} = 2.4**
$(\sin\theta/\lambda)_{max}$ (Å^{-1})	**0.651**
Range of h, k, l	**h = -8→8, k = -17→17, l = -14→14**
Refinement on	**F^2**
R[F^2 > 2σ(F^2)], wR(F^2), S	**0.050, 0.136, 1.02**
No. of reflections	**2148**
No. of parameters	**128**
No. of restraints	**0**
H-atom treatment	**H-atom parameters constrained**
Weighting scheme	**$w = 1/[\sigma^2(F_o^2) + (0.0727P)^2 + 0.0123P]$ where $P = (F_o^2 + 2F_c^2)/3$**
$(\Delta/\sigma)_{max}$	**< 0.001**
$\Delta\rho_{max}$, $\Delta\rho_{min}$ (e Å^{-3})	**0.17, -0.15**

Suitable X-ray quality crystals of the compound (**1**) were obtained after slow evaporation of the reaction mixture at room temperature. The crystallographic data and the structure refinement details of the title compound are listed in Table-1, while the selected bond lengths and bond angles are summarized in Table-2. The ORTEP view is shown in Fig. 4. In the title compound, the furan ring (O2/C8–C11) is oriented at a dihedral angle of 21.24 (11)° to the benzene ring (C1–C6). The bridge –C8—C7—N1—C6– torsion angle is -177.81 (15)°. All bond lengths and bond angles are normal (Table-2).

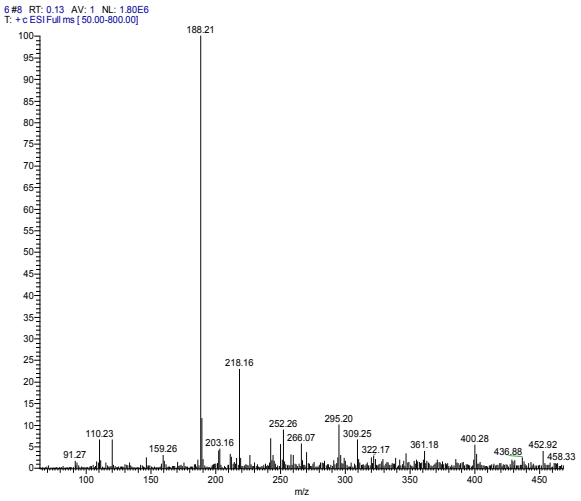

Fig. 3: Mass Spectrum of compound **1.**

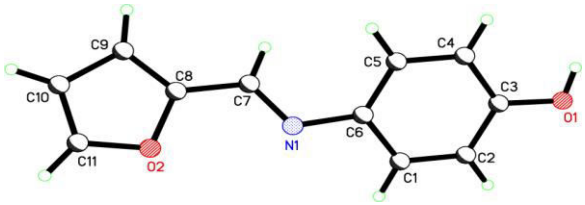

Fig. 4: ORTEP view of compound **1** with the atomic numbering scheme. Displacement ellipsoids for non-H atoms are drawn at the 50% probability level.

In the crystal, molecules are linked *via* intermolecular O—H...N and C—H...O hydrogen bonds, forming a 3D network (Table-3, Figs. 5-7).

Table-2: Selected geometric parameters (Å, º) for **1.**

Bond lengths			
O1-C3	**1.357 (2)**	**N1-C6**	**1.4211 (19)**
O2-C8	**1.371 (2)**	**N1-C7**	**1.275 (2)**
O2-C11	**1.352 (3)**		
Bond angles			
C8-O2-C11	**106.01 (19)**	**N1-C6-C1**	**117.07 (15)**
C6-N1-C7	**120.20 (14)**	**N1-C7-C8**	**122.82 (16)**
O1-C3-C4	**122.84 (16)**	**O2-C8-C9**	**110.46 (16)**
O1-C3-C2	**117.75 (15)**	**O2-C8-C7**	**118.66 (16)**
N1-C6-C5	**124.35 (15)**	**O2-C11-C10**	**110.7 (3)**

Table-3: Hydrogen-bond parameters (Å, °) for **1.**

D-H···A	**D-H(Å)**	**H···A(Å)**	**D···A(Å)**	**D-H···A(°)**
O1-H1A···N1^{i}	**0.8200**	**1.9600**	**2.7529(18)**	**163.00**
C7-H7···O1^{ii}	**0.9300**	**2.5500**	**3.19(2)**	**126.00**

Symmetry codes: (i) *x*+1/2, -*y*+1/2, *z*+1/2; (ii) *x*+1/2, -*y*+1/2, *z*-1/2

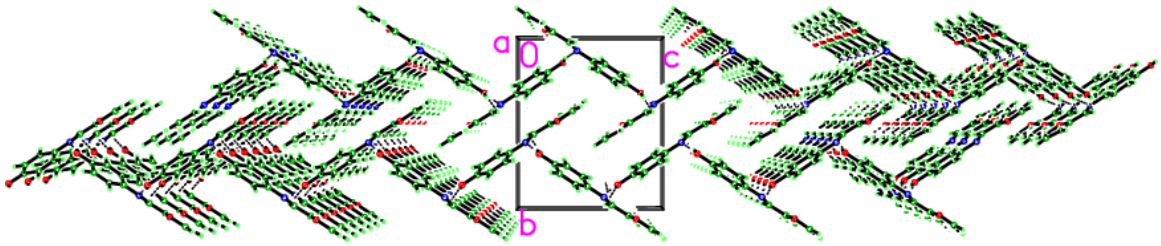

Fig. 5: Packing giagram of **1** viewed along a-axis making a 3D polymeric network like structure. Dotted lines show the intermolecular H-bonding.

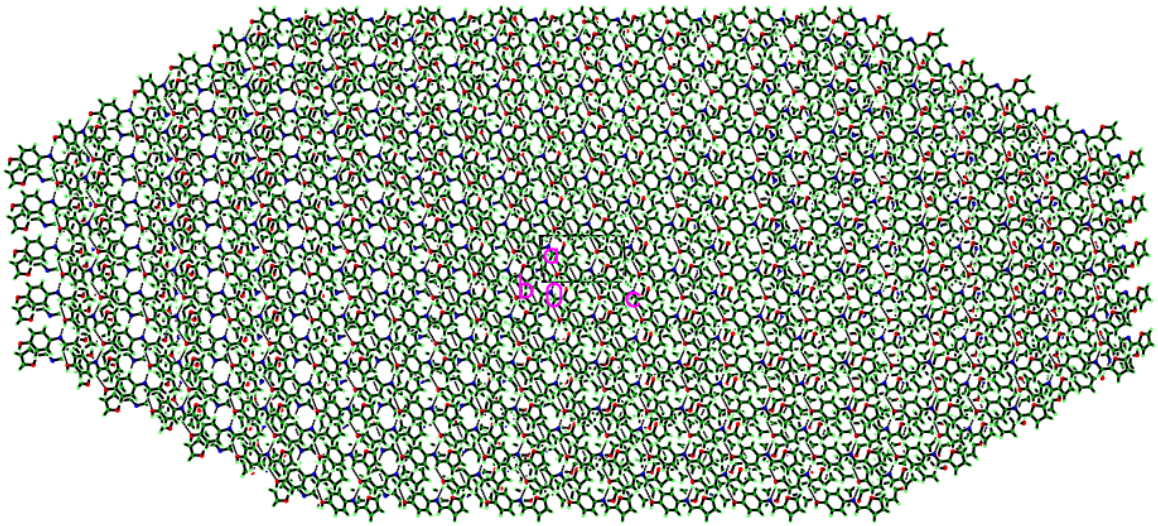

Fig. 6: Packing giagram of **1** viewed along b-axis making a wiregauze like structure. Dotted lines show the intermolecular H-bonding.

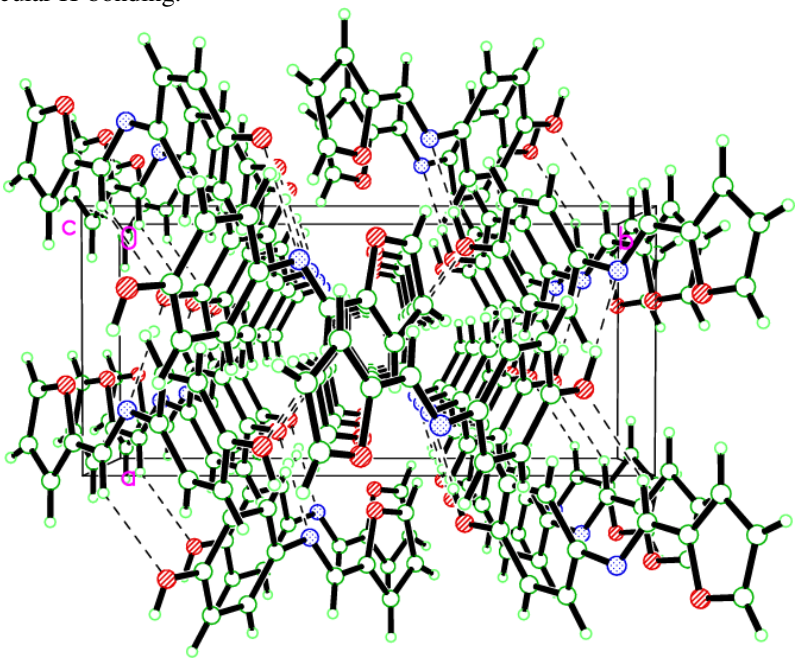

Fig. 7: Packing giagram of **1** viewed along c-axis making a spider like structure. Dotted lines show the intermolecular H-bonding.

Biological Activities

The target compound was evaluated for the biological activities against:

- Antifungal activity against fungal strain (*Fusarium oxysporum f.sp albedinis*) isolated from a date palm having a vascular fusariose.
- Anticancer activity against human cancer cell lines such as: breast (MDA-MB231) and colorectal (LoVo) cancers.

Antifungal Activity

The results revealed a significant activity against the fungal strain. Compounds bearing ($X^{\delta-}$----$Y^{\delta-}$) pharmacophore site are significantly active against fungal strains [11]. It is found that the negative charges of the sulfur and imine groups contribute positively in favor of an antifungal activity. The greater activity of pharmacophore site is due to the physicochemical properties and the ability of penetrating the fungal cell envelope and reach its cellular action site [19].

Table-4: IC_{50} values of compound **1** against breast and colorectal cancer cell lines.

Compound	MDA-MB231 IC_{50} (µg/mL)	LoVo IC_{50} (µg/mL)
1	6.9	14.6

Anticancer Activity

The anti-proliferative activity of the synthesized compound was studied against breast cancer cell lines and the data is shown in Table-5. This is evident by the IC_{50} values which present an inhibitory activity at micromolar concentration. The result is probably related to the high radical-scavenging property of hydroxyl group [20]. It is known that "free radicals" are omnipresent in our body and are generated by normal physiological processes. These radicals can inflict cellular damage which contributes to cancer [21]; several defenses have evolved both to protect our cells from radicals such as antioxidant scavengers. Indeed, the larger conjugate system, the higher radical-scavenging property and lower steric hindrance in the framework of hydroxyl-substituent Schiff base benefit these products to trap radicals [11]. This result highlights the interest of the present compound in the treatment of the radical-related disease.

Table-5: MIC values of compound **1** against *Fusarium oxysporum f. sp. Albedinis.*

Compound	20 µL	80 µL	160 µL	% Inhibition = (D°-Dx)/D° x 100			MIC (µg/mL)
1	3.5	1.2	0.8	30	76	84	128

POM Analyses of Compound **1**

The major issue concerned with synthetic drugs is the presence of various side effects. For a compound having the characteristics of a potential drug, besides having a good biological activity, must have good pharmacokinetic properties in biological systems. To access the pharmacokinetic profile of synthesized molecules, we used well established *in silico* methods such as Osiris, Petra and Molinspiration validated with about 7000 drug molecules available on the market [20-22].

The data of theoretical toxicity risks for compounds 1-6 calculated with the aid of the Osiris program are shown in Table-6. Sciff Base derivative (1) is supposed to present less risks when run through the mutagenicity, tumorigenicity assessments, and that these compounds are at limited risk comparable with standard synthetic drugs as near as irritation and reproductive effects are concerned. The hydrophilicity character of each compound has been expressed in terms its cLogP value since it has been established that the absorption or permeation is greatly affected by this quantity (value of cLogP). Accordingly, when the value of cLogP is higher than 5, the absorption or permeation decreases. Our results show that the compound has cLogP values within the acceptable criteria but need more chemical modification in order to make more potentially active analogues against various biotargets (GPCRL: GPCR ligand; ICM: Ion channel modulator; KI: Kinase inhibitor; NRL: Nuclear receptor ligand; PI: Protease inhibitor; EI: Enzyme inhibitor). The actual drug-score of 1 is very encouraging (0.43) as shown in Table-6. Thus, the cLogP and drug-score (DS) parameters should be taken into consideration and serve as a guide for further enzymatic screening investigations [20-22].

Table-6: Osiris calculations of compound **1.**

Compounds	Toxicity Risks [a]				Bioavailability and Drug-Score [b]				
	MUT	TUM	IRRIT	RE	MW	CLP	S	DL	D-S
1					187	1.88	-2.54	-1.61	0.43
STR[c]					581	-8.09	0.98	2.00	0.48

: not toxic ; : slightly toxic. a) MUT: mutagenic; TUM: tumorigenic; IRRIT: irritant; RE: reproductive effective. b) CLP: c*Log*P, S: Solubility, DL: druglikness, DS: Drug-Score. c) **STR**: Streptomycin (reference drug)

Table-7: Molinspiration calculations of compound **1.**

Compound	Molecular Properties [a]				Bioactivity Scores [b]					
	TPSA	ONH	VIOL	VOL	GPCR	ICM	KI	NRL	PI	EI
1	46	1	0	168	-1.17	-0.95	-1.15	-1.24	-1.47	-0.70
STR[c]	335	17	1	470	0.08	0.05	-0.23	-0.32	0.65	0.52

TPSA: Total of Polar surface area; ONH: OH-N or O-HN Interraction; VIOL: Violation of Lipinski rules; VOL: Volume. b) GPCR: GPCR ligand; ICM: Ion channel modulator; KI: Kinase inhibitor; NRL: Nuclear receptor ligamd; PI: Protease inhibitor; EI: Enzyme inhibitor. c) STR: Streptomycin (Reference drug)

The drug score combined drug likeness, cLogP, logS, molecular weight and toxicity risks in one handy value than may be used to judge the compound's overall potential qulification for a drug. This value is calculated by multiplying contributions of the individual properties with the equation (Eq. 1):

$$DS = \prod\left(\frac{1}{2}+\frac{1}{2}Si\right)\prod ti \qquad (Eq.\ 2)$$

where; S = 1/1 + eap + b.

DS is the drug score. Si is the contributions calculated directly from of cLog*P*; log*S*, molecular weight and drug likeness (pi) *via* the second equation, which describes a spline curve. Parameters a and b are (1, -5), (1, 5), (0.012, -6) and (1, 0) for cLog*P*, log*S*, molecular weight and drug likeness, respectively. "ti" is the contributions taken from the four toxicity risk types. The ti values are 1.0, 0.8 and 0.6 for no risk, medium risk and high risk, respectively. The reported compound **1** showed moderate to good drug score as compared with standard drugs used. The reported compound **1** showed important DS (DS = 0.43) which almost comparable to that of the standard drug used (DS = 0.48).

The heterocyclic arm can affect the bioactivity by influencing not only the electron density of the functional pharmacophore site but also its proper bioavailability. Number of violation of Lipinski 5 rules is neutral (NV = 0) as shown in Table-7. This let us do more and more modification on principal skeleten in goal to improve bioactivity [20-22].

Conclusion

The crystal structure of the title compound (**1**) with the furan ring oriented at a dihedral angle of 21.24(11)° to the benzene ring, is stabilized by intermolecular O—H...N and C—H...O hydrogen bonds, forming a 3D network. The greater activity of pharmacophore site is due to their physicochemical properties and their ability to penetrate the fungal cell envelope and reach its cellular action site. The newly synthesized compound should be more effective and possible act through a distinct mechanism from those of well-known classes of antimicrobial agents to which many clinically relevant pathogens are now resistant. The antifungal data clearly indicate that the compound has a strong antifungal activity and might be developed a new antifungal drug. The antifungal activity may be due to the interference with the function of parasite mitochondria. The activity of the synthesized comppound against the two cancer cell lines is probably due to the presence of hydroxyl group. Therefore, based on these activities the synthesized compound may be a beneficial and potential alternative and hence should be investigated further for the control of diseases.

Acknowledgements

The authors would like to extend their sincere appreciation to the Deanship of Scientific Research at king Saud University for its funding this Research group N° (RG -007-1435-1436).

Supplementary Information

Crystallographic data for the structural analysis has been deposited with the Cambridge crystallographic Data Centre, **CCDC# 981276** for compound (**1**). Copies of this information can be obtained free of charge from The Director, CCDC, 12 Union Road, Cambridge, CB2 1EZ, UK (fax: +44-1223-336033; e-mail: deposit@ccdc.cam.ac.uk or http://www.ccdc.cam.ac.uk).

References

1. M. Sirajuddin, N. Uddin, S. Ali and M. N. Tahir, Potential Bioactive Schiff Base Compounds: Synthesis, Characterization, X-Ray Structures, Biological Screenings and İnteraction with Salmon Sperm DNA, *Spectrochim. Acta Part A*, **116**, 111 (2013).
2. M. S. Karthikeyan, D. J. Parsad, B. Poojary, K. S. Bhat, B. S. Holla and N. S. Kumari, *Bioorg. Med. Chem*. **14**, 7482 (2006).
3. K. Singh, M. S. Barwa and P. Tyagi, Synthesis, characterization and biological studies of Co (II), Ni (II), Cu (II) and Zn (II) complexes with bidentate Schiff bases derived by heterocyclic ketone, *Eur. J. Med. Chem*. **411**, 147 (2006).
4. D. N. Dhar and C. L. Taploo, Schiff bases and their applications, *J. Sci. Ind. Res*. **41**, 501 (1982).
5. P. Przybylski, A. Huczynski, K. Pyta, B. Brzezinski and F. Bartl, Biological properties of Schiff bases and azo derivatives of phenols, *Curr. Org. Chem*. **13**, 124 (2009).

6. Y. Z. Tang and Z. Q. Liu, Quantitative structure–activity relationship of hydroxyl- substituent Schiff bases in radical- induced hemolysis of human erythrocytes, *Cell. Biochem. Funct*. **26**, 185 (2008).
7. Stoe & Cie. *X-RED32*, Darmstadt, Germany (2002).
8. G. M. Sheldrick, A short history of *SHELX, Acta Cryst.* **A64**, 112 (2008).
9. L. J. Farrugia, WinGX and ORTEP for Windows: an update, *J. Appl. Cryst.* **45**, 849 (2012).
10. A. L. Spek, **Si**ngle-crystal structure validation with the program PLATON, *J. Appl. Cryst*. **36**,7 (2003).
11. S. Radi, S. Tighadouini, O. Feron, O. Riant, Y. N. Mabkhot, S. S. Al-Showiman, T. Ben Hadda, M. El-Youbi, R. Benabbes and E. Saalaoui, One pot synthesis, antitumor, antibacterial and antifungal activities of some Schiff base heterocycles, *Int. J. Pharm*., **1**, 39 (2015).
12. S. Radi, Y. Toubi, N. Draoui, O. Feron and O. Riant, One Pot Synthesis and In Vitro Antitumor Activity of some Bipyrazolic Tripodal Derivatives, *Lett. Drug. Desig Discov*. **9**, 305 (2012).
13. L. P. Carrod and F. D. Grady, Antibiotics and Chemotherapy. 3rd ed., Churchill Livingstone, Edinburgh, p. 447 (1972).
14. M. Sirajuddin, S. Ali, V. Mckee, S. Zaib and J. Iqbal, Organotin(IV) carboxylate derivatives as a new addition to anticancer and antileishmanial agents: Design, physicochemical characterization and interaction with Salmon sperm DNA, *RSC Adv*. **4**, 57505 (2014).
15. J. Sheikh and T. Ben Hadda, Antibacterial, antifungal and antioxidant activity of some new water-soluble β-diketones, *Med. Chem. Res*. **22**, 964 (2013).
16. M. Sirajuddin, S. Ali, A. Haider, N. A. Shah, A. Shah and M. R. Khan, Synthesis, characterization, biological screenings and interaction with calf thymus DNA as well as electrochemical studies of adducts formed by azomethine [2-((3,5- dimethylphenylimino) methyl)phenol] and organotin(IV) Chlorides, *Polyhedron*, **40**, 19 (2012).
17. M. Sirajuddin, S. Ali, N. A. Shah, M. R. Khan and M. N. Tahir, Synthesis, characterization, biological screenings and interaction with calf thymus DNA of a novel azomethine 3-((3,5-dimethylphenylimino)methyl)benzene-1,2-diol *Spectrochim. Acta, Part A*, **94**, 134 (2012).
18. M. Sirajuddin, S. Ali, F. A. Shah, M. Ahmad and M. N. Tahir, Potential bioactive vanillin-Schiff base di- and tri-organotin(IV) complexes of 4-((3,5-dimethylphenylimino)methyl)-2-methoxyphenol: Synthesis, characterization and biological screenings, *J. Iran. Chem. Soc*. **11**, 297 (2014).
19. Y. Z. Tang and Z-Q. Liu, Quantitative structure–activity relationship of hydroxyl-substituent Schiff bases in radical-induced hemolysis of human erythrocytes, *Cell Biochem. Funct*. **26**: 185 (2008).
20. S. P. Hussain, L. J. Hofseth and C. C. Harris, Radical causes of cancer, *Nature Rev. Cancer*, (2003) *3*: 276.
21. M. Sirajuddin, S. Ali, V. McKee and H. Ullah, Synthesis, spectroscopic characterization, biological screenings, DNA binding study and POM analyses of transition metal carboxylates, *Spectrochim. Acta Part A*, **138**, 569 (2015).
22. N. Uddin, M. Sirajuddin, N. Uddin, M. Tariq, H. Ullah, S. Ali, S. A. Tirmizi and A. R. Khan, Synthesis, spectroscopic characterization, biological screenings, DNA binding study and POM analyses of transition metal carboxylates, *Spectrochim. Acta Part A*, **140**, 563 (2015).
23. T .B. Hadda, M. A. Ali, M. Vasand, S. Gharby, T. Fergoug and I. Warad, Tautomeric origin of dual effects of N_1-nicotinoyl-3-(4′-hydroxy-3′-methyl phenyl)-5-[(sub)phenyl]-2-pyrazolines on bacterial and viral strains: POM analyses as new efficient bioinformatics platform to predict and optimize bioactivity of drugs, *Med. Chem. Res*. **22**, 1438 (2013).